Journal of The Electrochemical Society, **164** (4) D196-D203 (2017)
0013-4651/2017/164(4)/D196/8/$37.00 © The Electrochemical Society

Copper Electroplating with Polyethylene Glycol

I. An Alternative Hysteresis Model without Additive Consumption

Hongliu Yang,[a,z] Arezoo Dianat,[a] Manfred Bobeth,[a] and Gianaurelio Cuniberti[a,b,c]

[a]*Institute for Materials Science and Max Bergmann Center of Biomaterials, 01062 Dresden, Germany*
[b]*Dresden Center for Computational Materials Science (DCCMS), TU Dresden, 01062 Dresden, Germany*
[c]*Center for Advancing Electronics Dresden (cfAED), 01062 Dresden, Germany*

Additives play an important role in electrochemical deposition and understanding their working mechanism is a great challenge. In cyclic voltammetry measurements of copper deposition, hysteresis is ubiquitously observed. Correct prediction of hysteresis behavior is an important test for deposition models. In previous models, including poly(ethylene glycol) (PEG) and chloride ions as additives, a common assumption to explain the hysteresis is the consumption of additives during copper deposition. However, second-ion mass spectrometry measurements often detected comparatively low levels of impurities in deposits. Therefore, we propose here an alternative mechanism for explaining hysteresis curves without invoking additive consumption. Essential ingredients of our models are: (i) a strongly nonlinear dependence of the maximal possible PEG coverage on the chloride coverage on the copper surface, (ii) a nonlinear dependence of the deposition current on the PEG surface coverage, and (iii) an additional activation of the desorption of additives with increasing copper deposition current. We demonstrate that our model reproduces characteristic features of cyclic voltammograms measured under vastly different conditions and exhibiting pronounced hysteresis. Furthermore, simulations are compared well to PEG adsorption/desorption experiments with varying additive concentrations. The proposed model may serve to describe deposition situations with negligible additive consumption.
© 2017 The Electrochemical Society. [DOI: 10.1149/2.1051704jes] All rights reserved.

Manuscript submitted December 16, 2016; revised manuscript received January 20, 2017. Published February 15, 2017.

Electrochemical deposition is a standard method in semiconductor industry to fabricate for instance metallic interconnects in integrated circuits.[1,2] With increasing level of integrity and scaling down of the chip size it becomes more and more difficult to achieve a void-free filling of trenches and vias for highly complex chip designs. Properly chosen additives are used to control the copper deposition by selectively suppressing or accelerating the deposition at specific locations of features. Understanding the working mechanisms of additives is of great importance to tailor a suited electrolyte-additive system to a given deposition task.

For copper plating in highly acidic electrolytes, the role of chloride ions and poly(ethylene glycol) (PEG) as additives has been extensively studied. Chloride ions in the electrolyte were found to enhance the copper deposition. The ions adsorb on the cathode surface within the applied potential range. The association of adsorbed chloride ions with cupric ions Cu^{2+} in the electrolyte enables an inner sphere electron transfer, which serves as an additional path for the reduction of Cu^{2+}.[3] PEG alone normally shows only negligible suppression of copper deposition. In the presence of both chloride ions and PEG, the copper deposition current can be reduced by about two orders of magnitude. Kelly and West's study[4] (using quartz crystal microbalance) indicates that PEG adsorbs on top of a chloride-covered copper surface, while on a bare copper surface (without chloride) adsorption of PEG was hardly detected. This was also confirmed by the in situ ellipsometry study of Walker et al.[5] It is commonly accepted that the coadsorption of PEG and Cl^- and formation of PEG-Cl complexes on the cathode surface prevent further approach of Cu^{2+} to the cathode and inhibit therefore copper deposition. Dow et al.[6] found that the degree of deposition suppression depends on the molecular weight of PEG. This finding further supports the picture that the deposition suppression is caused by the PEG-Cl coverage of the cathode surface. Note that there are also discussions whether copper ions take part in the PEG adsorption and corresponding deposition suppression.[7,8]

To characterize the electrochemical properties of electrolytes for copper plating, cyclic voltammograms (CVs) are commonly measured. In the case of electrolytes with PEG and Cl^- additives, CVs frequently exhibit a hysteresis.[9–14] This means that the deposition current varies differently for forward and backward sweeping of the potential. Along with a hysteresis, a sudden change from a low-current to a high-current state often occurs during the forward (cathodic direction) sweeping, see for instance Fig. 1 of Ref. 13. For a fixed PEG concentration of 1 mM, Jovic and Jovic[9] increased the Cl^- concentration from 0.001 up to 1 mM and observed a transition in the CVs from an unsuppressed deposition to a highly suppressed one. For intermediate Cl^- concentrations, the CVs showed a hysteresis.[9] Wu et al.[10] fixed the concentration of Cl^- at 2.174 mM and considered the PEG concentrations 10^{-7}, 10^{-6} and 10^{-5} M. Hysteresis was observed for the two cases with lower PEG concentrations. Using post-experiment compensation for the potential drop in electrolyte Moffat and Josell[15] found an S-shaped negative differential resistance (S-NDR) behavior, which indicates the existence of bistable states for a range of overpotential. The appearance of hysteresis is therefore not due to a finite sweeping rate, but rather owing to the intrinsic nonlinearity of the system dynamics. A similar S-NDR behavior was previously observed for the deposition of Zn and Ni as well.[16,17] Also, bottom-up superfilling of high-aspect-ratio through-silicon vias (TSV) was achieved by using the simple additive system with only PEG and Cl^-.[15,18,19] At the top and side wall of the vias, copper deposition was almost completely suppressed while at the via bottom a nearly unsuppressed deposition occurred. The above-mentioned findings bring renewed interest in the working mechanisms of such a simple additive system. In this respect, the correct prediction of the hysteresis of CVs may be considered as a sensitive test of copper deposition models.[13,14,20]

Modeling of electrochemical copper deposition is important for the understanding of additive systems and for a cost-effective screening and optimization of deposition conditions. Although in production applications PEG and Cl are commonly used together with the accelerator additive SPS, studying the sole PEG-Cl system in a first step is naturally fundamental to understand the whole SPS-PEG-Cl system, where the interplay between SPS and PEG is crucial.[22–24,27,28] Moreover, the achievement of the superfilling of TSVs in a PEG-Cl bath without SPS[15] points to the technical importance of this system and further motivates its study. In the past, extensive modeling efforts were already devoted to the effect of PEG and Cl^-. Some of those models also describe the hysteresis behavior.[11–14,18,19,21,25,26] A common assumption to explain the hysteresis (except in Ref. 14) is the consumption of additives during copper deposition. The consumption may be due to their incorporation in the deposit or their degradation. By means of secondary-ion mass spectrometry, Kang and Gewirth[29] found that the incorporation rate of PEG and Cl^- in the deposited copper is very low. To reproduce the measured CVs within a deposition model, a much larger consumption rate has to be supposed. In this respect, a stochastic model without additive incorporation in the deposit was recently introduced by Yang et al.[14] This model considers

[z]E-mail: hongliu.yang@tu-dresden.de

Downloaded on 2017-06-29 to IP 141.30.233.235 address. Redistribution subject to ECS terms of use (see ecsdl.org/site/terms_use) unless CC License in place (see abstract).

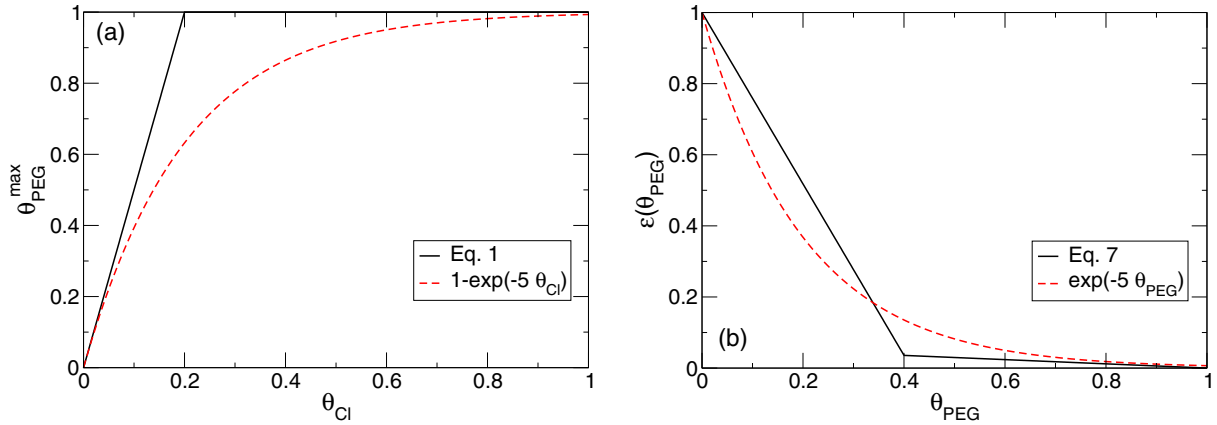

Figure 1. (a) Coverage-capacity function $\theta^{max}_{PEG}(\theta_{Cl})$, which is the maximally possible surface coverage of PEG for a given chloride surface coverage ($\theta^{*}_{Cl} = 0.2$), and (b) the suppression function $\epsilon(\theta_{PEG})$, characterizing the current suppression in dependence on the PEG surface coverage ($\theta^{*}_{PEG} = 0.4$). Solid lines represent the piecewise-linear case according to Eqs. 1 and 7. Dashed lines show a smooth variation of the two functions.

the multi-step co-adsorption and desorption of PEG and chloride on copper and is able to reproduce their experimental measurements, especially the hysteresis of CVs. To summarize, previous models (except Ref. 14), which are able to explain the hysteresis behavior, rely on the assumption of additive consumption. However, the latter is in contrast to the very high copper film purity measured. This unsatisfactory situation motivated us to propose in the present work a new modeling approach to explain hysteresis without additive consumption.

Our new model follows the lines of Yang et al.[14] and takes into account, for the first time, the strongly nonlinear dependence of the suppression of copper deposition on the PEG surface coverage. This dependence is inferred from the PEG desorption experiments of Willey and West.[31] Moreover, instead of the detailed description of the multi-step co-adsorption kinetics in Ref. 14 we introduced in our model a nonlinear function to relate the maximally possible PEG surface coverage to a given chloride coverage. Despite the omission of additive consumption, the model is able to reproduce a series of characteristic features of CVs, measured under vastly different deposition conditions, as well as of special PEG adsorption and desorption experiments. In this way, we attempt to contribute in elucidating the factors, which are crucial for the deposition suppression by PEG and Cl^-,

In the following section, we present our modeling approach in detail. The predictive power of our model is then demonstrated by simulating various characteristic CVs and PEG adsorption experiments, which have been reported in the literature. Furthermore, we discuss the effect of different model parameters on the the copper deposition rate.

Model

PEG-Cl^- coadsorption.—In view of the experimental observations found by crystal microbalance[4] and in situ ellipsometry,[5] we suppose here that PEG adsorbs only on top of a Cl^--covered copper surface, ignoring PEG adsorption on the bare surface. In view of the abundance of copper ions, we will not consider them explicitly in the following discussion of the additive complex. Taking into account the large size of PEG molecules compared to Cl^- ions, multiple binding sites between one PEG molecule and adsorbed Cl^- ions should exist.[26] We assume a PEG molecule being adsorbed if a certain minimal number of bonds with adsorbed Cl^- ions are formed. This means that complete PEG coverage can be reached already at a certain threshold value of the Cl^- surface coverage $\theta^{*}_{Cl} < 1$. Correspondingly, the following relationship between the maximally possible surface coverage of PEG, θ^{max}_{PEG}, and the Cl^- coverage θ_{Cl} is postulated (see Fig. 1)

$$\theta^{max}_{PEG}(\theta_{Cl}) = \begin{cases} \theta_{Cl}/\theta^{*}_{Cl}, & \text{if } \theta_{Cl} \le \theta^{*}_{Cl} \\ 1.0. & \text{otherwise} \end{cases} \quad [1]$$

This relationship will be referred to as coverage-capacity function in the following.

The Cl^- coverage results as competition between Cl^- adsorption and desorption processes. In addition to the thermally activated desorption of Cl^-, we assume Cl^- desorption to be activated also by copper deposition. Although the detailed atomistic mechanisms are unclear, it seems likely that copper deposition as an exothermic process will excite the thermal motion of neighboring chloride ions. A higher copper deposition rate corresponds to a larger release of latent energy and, in consequence, to a larger desorption rate of additives. A current-dependent desorption rate of additives was also proposed in Ref. 14, based on the argument of faster morphological changes of the copper surface with increasing deposition current.

The adsorption-desorption kinetics of additives on the cathode surface can be described by the following modified Langmuir model

$$\Gamma_{Cl}\frac{d\theta_{Cl}}{dt} = k^{Cl}_{A} c_{Cl}(1-\theta_{Cl}) - k^{Cl}_{D}\theta_{Cl}, \quad [2]$$

and

$$\Gamma_{PEG}\frac{d\theta_{PEG}}{dt} = k^{PEG}_{A} c_{PEG}(\theta^{max}_{PEG} - \theta_{PEG}) - k^{PEG}_{D}\theta_{PEG}, \quad [3]$$

with

$$k^{Cl}_{D} = k^{Cl}_{D,0} + k_c (i_{Cu})^{\beta}, \quad [4]$$

where Γ_i are the surface concentrations (in mole/m^2) at saturation, k^i_A and k^i_D are the adsorption and desorption rate constants, c_i are the concentrations, and θ_i the surface coverages of the two additives i = PEG and Cl^-, respectively. i_{Cu} is the deposition current density of copper. The last term in Eq. 4 represents the contribution to the Cl^- desorption rate which is due to the additional activation of Cl^- desorption caused by copper deposition. For the desorption of PEG, a similar term could be included in Eq. 3, but no essential changes in the model behavior were observed. Thus, for simplicity, we omit such a term in Eq. 3. We tested different values of the exponent β in Eq. 4, namely 0.5, 1.0, and 2.0. Since all values gave similar results, we use $\beta = 1$ in the following.

Deposition suppression.—The deposition current of copper as a function of the applied potential is commonly described by the Butler-Volmer-like equation

$$i_{Cu} = i_0 \frac{c_{Cu}}{c^{b}_{Cu}} \left\{ e^{\frac{(1-\alpha)F\eta}{RT}} - e^{-\frac{\alpha F\eta}{RT}} \right\}, \quad [5]$$

where c_{Cu} and c^b_{Cu} are the concentrations of copper ions at the cathode surface and in the bulk solution, respectively, and i_0 is the exchange current density.[9,26]

Downloaded on 2017-06-29 to IP 141.30.233.235 address. Redistribution subject to ECS terms of use (see ecsdl.org/site/terms_use) unless CC License in place (see abstract).

To mimic the suppression effect of PEG-Cl complexes, the following simple formula for the exchange current density was proposed in Ref. 21: $i_0^{PEG} = \epsilon i_0^{free}$ where i_0^{free} corresponds to the additive-free surface and i_0^{PEG} to the PEG covered surface ($\epsilon < 1$). In consequence, the exchange current density becomes a linear function of the PEG surface coverage, $i_0 = i_0^{free}(1 - \theta_{PEG}) + i_0^{PEG}\theta_{PEG} = i_0^{free}(1 - (1 - \epsilon)\theta_{PEG})$, which has often been used in previous simulations.

The adsorption-desorption behavior of PEG was studied by Willey and West using a microfluidic electrochemical cell.[31] After immersing a PEG-saturated cathode into an additive-free electrolyte, the copper deposition current shows a very slow linear increase in the initial stage, followed by a fast exponential increase in a second stage. From such transient measurements, the authors inferred that the PEG adsorption-layer initially becomes only thinner, possibly via configuration rearrangements of adsorbed PEG molecules. Afterwards, when the amount of adsorbed PEG is below a certain threshold value, the adsorption layer becomes patchy in a second desorption stage, i.e. empty spaces between adsorbed PEG molecules appear on the copper surface (cf. also discussion and illustrations in Ref. 31). Based on this two-stage PEG desorption behavior, together with our reasoning in the Appendix, we suggest the following description of the current suppression by PEG-Cl complexes

$$i_0 = \epsilon(\theta_{PEG}) i_0^{free}, \qquad [6]$$

with the function

$$\epsilon(\theta_{PEG}) = \begin{cases} 1 - (1 - \epsilon_1)\frac{\theta_{PEG}}{\theta^*_{PEG}}, & \text{if } \theta_{PEG} \le \theta^*_{PEG} \\ \epsilon_0 - (\epsilon_0 - \epsilon_1)\frac{1-\theta_{PEG}}{1-\theta^*_{PEG}}, & \text{otherwise} \end{cases} \qquad [7]$$

where θ^*_{PEG} is the threshold PEG-coverage below which the adsorption layer becomes patchy. In view of the complex adsorption-desorption behavior of PEG (see e.g[31]), the quantity θ_{PEG} should be understood as the normalized surface density of adsorbed PEG. For brevity, it will be referred to as surface coverage of PEG in the following, and the function $\epsilon(\theta_{PEG})$ will be referred to as suppression function. As shown in Fig. 1, this function is a piecewise-linear function of the PEG surface coverage. As will be demonstrated below, this special non-linearity of the suppression function is crucial for the occurrence of hysteresis of CVs in our proposed model.

Transport equations.—The mass transport of copper ions and additives to the cathode surface occurs mainly by diffusion, convection and, for charged species, also by migration, driven by the electric field. In the case of a rotating disk electrode, the corresponding transport problem has been analyzed in detail in Ref. 32. It was found that diffusion is important within a so-called diffusion layer above the cathode surface. Outside the diffusion layer, one can approximately assume that the concentrations of copper ions and additives c_i are uniform and equal to their bulk values c_i^b. Within the diffusion layer, copper ions and additives are transported in normal z-direction to the cathode surface via diffusion and convection, described by the equations

$$\frac{\partial c_i}{\partial t} = D_i \frac{\partial^2 c_i}{\partial z^2} - v \frac{\partial c_i}{\partial z}, \qquad [8]$$

where D_i is the diffusivity of copper ions or additives and v the normal velocity of the fluid (directed to the surface), which is caused by the rotation of the disk electrode. According to the Levich theory,[32] the thickness of the diffusion layer L_{diff} and the normal velocity v depend on the diffusivity D, the rotation velocity of the electrode ω, and the viscosity of the electrolyte ν: $L_{diff} = 1.61 D^{1/3}\omega^{-1/2}\nu^{1/6}$ and $v = -0.51\omega^{3/2}\nu^{-1/2}z^2$. Here, the diffusivity of the fastest species, copper, is used to determine the value of L_{diff}. For simplicity, the migration term for charged species is omitted in Eq. 8 since our simulation results showed that this term is negligible compared to the diffusion and convection terms. The boundary conditions for the concentrations read

$$c_i|_{z=L_{diff}} = c_i^b, \qquad [9]$$

and at the cathode surface

$$D_i \frac{\partial c_i}{\partial z}|_{z=0} = \Gamma_i \frac{d\theta_i}{dt} \qquad [10]$$

for i = PEG, Cl, and for copper

$$-D_{Cu}\frac{\partial c_{Cu}}{\partial z}|_{z=0} = \frac{i_{Cu}}{2F}. \qquad [11]$$

The above system of coupled equations for the concentrations c_i with i = Cu, PEG, Cl and the surface coverages θ_i with i = PEG and Cl was solved numerically via a backward-time centered-space finite difference method for given values of c_i^b and the cathode overpotential η. To check the accuracy of the finite-difference code, the simulation results have been compared with calculations using the finite-element software Comsol.

Table I. Parameter values used in the simulations.

Parameter	Value	Unit	Source
L_{diff}	1.5×10^{-4}	m	This work
c^b_{Cu}	250	mole/m^3	This work
sweep rate	5×10^{-4}	V/s	This work
D_{Cu}	5×10^{-10}	m^2/s	Ref. 26
D_{Cl}	2×10^{-9}	m^2/s	Ref. 13
D_{PEG}	1×10^{-10}	m^2/s	Ref. 13
Γ_{Cl}	1.3×10^{-5}	mole/m^2	Ref. 26
Γ_{PEG}	2.67×10^{-7}	mole/m^2	Ref. 13
α_c	0.46		Ref. 26
i_0^{free}	7.7	A/m^2	Ref. 26
k_A^{Cl}	1.8×10^{-6}	m/s	Ref. 26
$k_{D,0}^{Cl}$	$k_{Cl}^A/200$	mole/m$^2 \cdot$ s	Ref. 26
k_A^{PEG}	3.6×10^{-8}	m/s	This work
k_D^{PEG}	$k_A^{PEG}/25$	mole/m$^2 \cdot$ s	This work
k_c	3.9×10^{-8}	mole/m$^2 \cdot$ A	This work
θ^*_{Cl}	0.2		Ref. 26
θ^*_{PEG}	0.4		This work
β	1.0		This work
ϵ	0.0357		Ref. 26

Results and Discussion

To demonstrate the predictive power of our model, we have performed numerous simulations and compared them with experiments reported in the literature, especially with experiments concerning the adsorption of additives as well with CV measurements showing a hysteresis. The parameters used in our simulations are listed in Table I. Largely, they have been found in the literature. In view of the large scatter of kinetic parameters for additive adsorption, being extracted from different experiments, we had to choose consistent values for those parameters. For the adsorption and desorption rate constants of chloride, we used values reported in Ref. 26. For PEG, in view of its large molecule size compared to chloride, we assumed a considerably smaller adsorption rate constant.

For our purpose of a mechanistic study of the role of additives, such a parameter setting should be sufficient. As shown below, it illustrates quite well the capability of our model and even facilitates the qualitative comparison with experiments performed under vastly different conditions. For a quantitative comparison with measurements, the model parameters need to be fitted to specific experiments, which currently is in progress and will be reported elsewhere.

PEG Adsorption-desorption kinetics.—As a first test of our proposed model, we simulated experiments by Willey et al.[31] which concerned the desorption of PEG in the presence of chloride in the electrolyte. The copper deposition current was observed over time

Downloaded on 2017-06-29 to IP 141.30.233.235 address. Redistribution subject to ECS terms of use (see ecsdl.org/site/terms_use) unless CC License in place (see abstract).

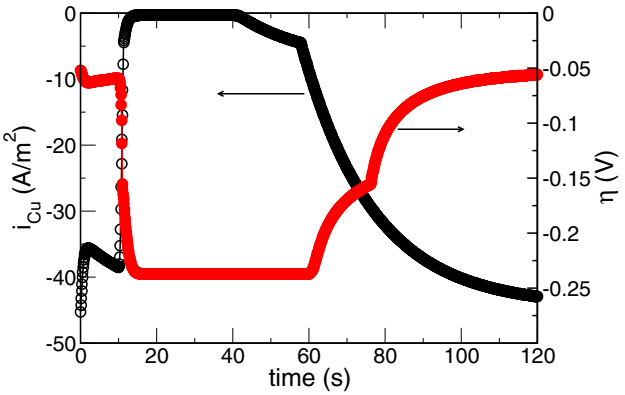

Figure 2. Simulation of the deposition current vs time to explore the PEG desorption, similar to experiments reported in Ref. 31. PEG of concentration 1 mM was injected into the electrolyte at 10 s, and removed at 40 s and 60 s under potentiostatic and galvanostatic conditions, respectively. In both cases, PEG desorption proceeds in two stages with different speeds in qualitative agreement with the measurements in Ref. 31, Figure 2. Parameters: $c_{Cl} = 0.1$ mM, $\eta = -0.1$ V (potentiostatic), $i = -20$ A/m^2 (galvanostatic), diffusion layer thickness $L_{diff} = 10$ µm according to the conditions in Ref. 31.

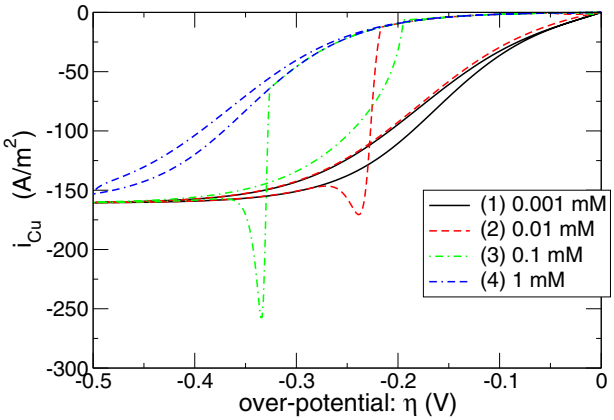

Figure 4. Simulation of CVs for different Cl^- concentrations $c_{Cl} = 0.001$, 0.01, 0.1, 1 mM ($c_{PEG} = 1$ mM). The curves reveal a strong current suppression at high Cl^- concentration of 1 mM and nearly no suppression at 0.001 mM. For intermediate concentrations, a pronounced hysteresis is found. A qualitatively similar behavior was found experimentally in Ref. 26, Fig. 1, and in Ref. 14, Fig. 8.

under potentiostatic condition. At a time of $t = 10$ s, PEG of concentration 1 mM was injected into the electrolyte and removed at $t = 40$ s (cf. Fig. 2). Analogously, under galvanostatic condition, the cathode overpotential was measured, where PEG was removed at $t = 60$ s. In agreement with the measurements of Willey et al., PEG adsorption and corresponding suppression of the current (potentiostatic case) occur very fast. The desorption of PEG is considerably slower and proceeds in two stages. For the potentiostatic case, a nearly linear decrease of the deposition current is followed by a steep exponential one. The successful qualitative reproduction of the experimental results of Willey et al.,[31] especially the two-stage desorption of PEG, supports the plausibility of our proposed description of the current suppression by PEG-Cl complexes in Eq. 7.

Further simulations were performed to elucidate the dependence of the suppression of copper deposition on the PEG concentration. To this end, the deposition current over time after PEG injection (at $t = 50$ s) was calculated, see Fig. 3. The curves reveal that for high PEG concentration (0.1 to 1 mM) a strongly suppressed deposition state is rapidly reached, whereas for low concentration of 0.02 mM a considerably less suppressed state is reached only after about 100 s. The curves in Fig. 3 are in qualitative agreement with measurements by Willey et al.[31] This may be considered as a further support of our model assumptions, especially for the suppression function $\epsilon(\theta_{PEG})$ in Eq. 7.

Cyclic voltammetry.—The simulations in Fig. 4 demonstrate how the current suppression by additives changes with increasing chloride concentration, while the PEG concentration is fixed at a sufficiently high value of $c_{PEG} = 1$ mM. For a Cl^- concentration of $c_{Cl} = 0.001$ mM, the deposition current is hardly suppressed, while a full suppression is observed for $c_{Cl} = 1$ mM. For those two cases, the forward (cathodic direction) and backward potential scans take almost identical paths. In contrast, for $c_{Cl} = 0.01$ mM and 0.1 mM, the forward scan first follows the branch of full suppression and suddenly jumps with some overshooting to the unsuppressed branch at a critical potential. The backward scan follows the unsuppressed branch even after crossing the critical potential. For $c_{Cl} = 0.1$ mM, it gradually returns then to the full-suppression branch. Corresponding experimental studies of the influence of the Cl^- concentration on the CVs are reported for example in Ref. 26, Fig. 1, and in Ref. 14, Fig. 8a. In those studies, CVs with hysteresis and a steep current increase during the forward scan were observed, similar to the present simulations.

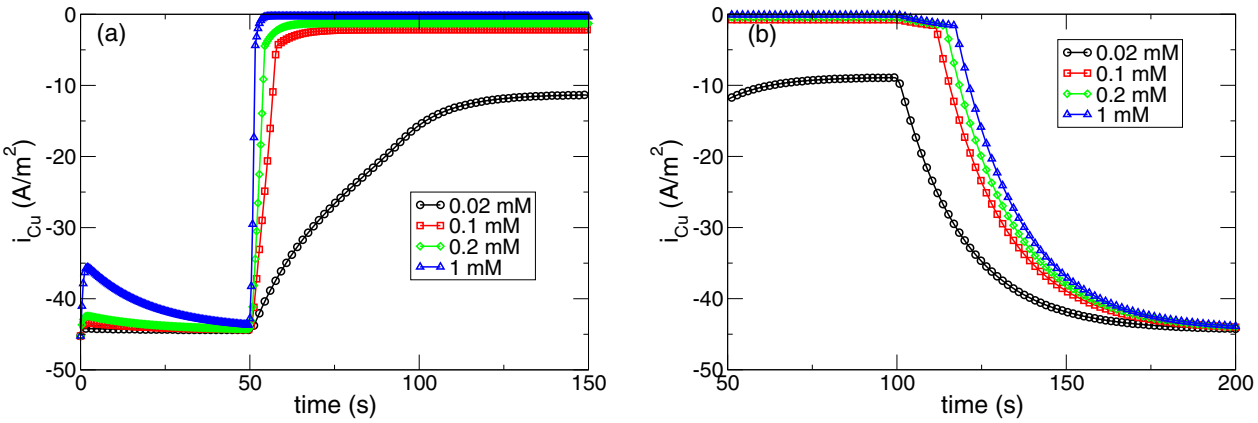

Figure 3. Simulations of the deposition current vs time during potentiostatic adsorption (a) and desorption (b) of PEG for different PEG concentrations $c_{PEG} = 0.02, 0.1, 0.2, 1$ mM ($c_{Cl} = 0.1$ mM, $\eta = -0.1$ V). PEG was injected into the electrolyte at $t = 50$ s for the simulation in (a) and removed at $t = 100$ s for that in (b). Adsorption strongly slows down for the small PEG concentration and the saturation coverage decreases significantly. Remarkably, the desorption curves show a two-stage behavior at higher PEG concentrations, starting with a slow desorption stage. A qualitatively similar behavior was experimentally observed, cf. Figs. 4 and 8 of Ref. 31.

Downloaded on 2017-06-29 to IP 141.30.233.235 address. Redistribution subject to ECS terms of use (see ecsdl.org/site/terms_use) unless CC License in place (see abstract).

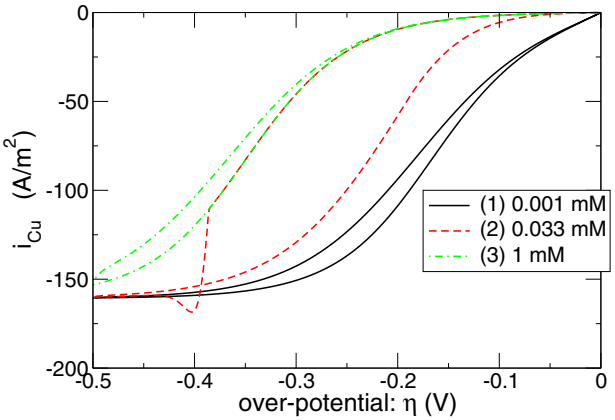

Figure 5. Simulation of CVs for different PEG concentrations $c_{PEG} = 0.001$, 0.033, 1 mM ($c_{Cl} = 0.3$ mM). The curves reveal a highly-suppressed deposition current at high PEG concentration. For the intermediate concentration, a jump-like transition from this highly-suppressed state to the unsuppressed state takes place with increasing negative cathode potential. Hysteresis is most pronounced at this intermediate concentration. Similar experimental measurements have been reported in Ref. 10, Fig. 6.

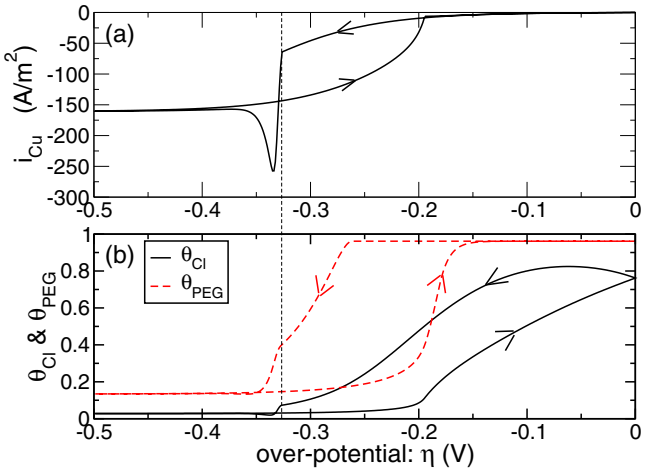

Figure 7. Simulation of the deposition current density i_{Cu} (a) as well as the surface coverages of PEG and chloride (b) as functions of the overpotential ($c_{Cl} = 0.1$ mM, $c_{PEG} = 1$ mM, $\theta^*_{Cl} = 0.2$, $\theta^*_{PEG} = 0.4$). The steep change in the current density i_{Cu} starts when the surface coverage of PEG θ_{PEG} crosses the value $\theta^*_{PEG} = 0.4$.

For the complementary case of varying PEG concentration $c_{PEG} = 0.001$, 0.033, 1 mM and fixed Cl^- concentration $c_{Cl} = 0.3$ mM, simulations of CVs are presented in Fig. 5. The simulated CVs exhibit a transition from an unsuppressed state to a highly suppressed one with increasing PEG concentration. Furthermore, hysteresis is observed for the intermediate PEG concentration in qualitative agreement with experimental measurements presented in Ref. 10, Fig. 6.

Effect of PEG molecular weight.—Measurements by Yang et al.[14] revealed that the hysteresis behavior of CVs is also effected by the molecular weight of PEG. To analyze the impact of the molecular weight of PEG on the current suppression within our model, we adjusted the value of θ^*_{Cl} according to different molecular weights. This adjustment is based on the limiting assumption that a fixed number n^* of bonds between one PEG molecule and adsorbed Cl^- ions is sufficient to keep a PEG molecule in the adsorbed state on the copper surface, independent of its molecular weight. The threshold value θ^*_{Cl} results then as the ratio n^*/n_{tot}, where n_{tot} is the total number of Cl^- adsorption sites on the copper surface within the contact area between the PEG molecule and the copper surface. This implies that θ^*_{Cl} is inversely proportional to the PEG contact area, which in turn is related to its molecular weight M_{PEG}. Following Kelley and West,[4] we assume here a semi-spherical shape of adsorbed PEG molecules. Then, the contact area is proportional to $M^{2/3}_{PEG}$ and, consequently, θ^*_{Cl} is proportional to $M^{-2/3}_{PEG}$. Thus, a smaller value of θ^*_{Cl} corresponds to a higher molecular weight. Fig. 6 shows simulations of CVs for the two values $\theta^*_{Cl} = 0.2$ and 0.4, corresponding to a weight ratio of PEG molecules of 2.83 ($c_{Cl} = 0.1$ mM). In order to compare two electrolyte systems with the same mass concentration of PEG, the bulk molecule concentration was adjusted correspondingly (for $\theta^*_{Cl} = 0.4$ the bulk concentration is larger by the factor 2.83). Owing to the change of the surface area of a single PEG molecule with θ^*_{Cl}, the molar surface concentration at saturation for the case with $\theta^*_{Cl} = 0.4$ was doubled. As can be seen in Fig. 6, for larger molecular weight ($\theta^*_{Cl} = 0.2$), the transition from the suppressed to the unsuppressed state occurs at a more cathodic potential. This tendency has also been found in the experiments by Yang et al.,[14] Fig. 10a. Their measured CVs show, however, no overshooting, which could be related to the considerably higher electrode rotation velocity used in their experiment.

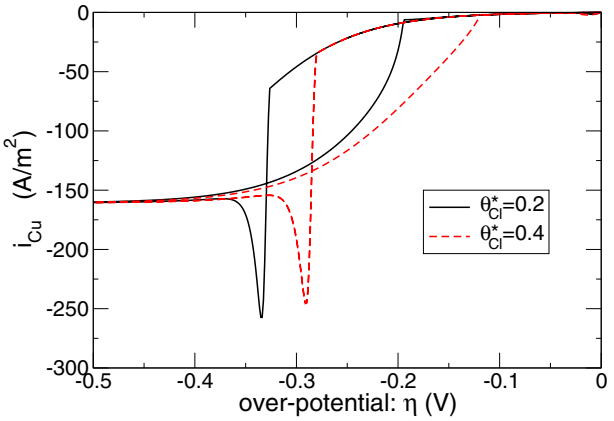

Figure 6. Simulation of CVs to elucidate the effect of the model parameter θ^*_{Cl}, which is thought to be closely related to the molecular weight of PEG. With increasing molecular weight, θ^*_{Cl} should diminish (parameters: $\theta^*_{Cl} = 0.2$, 0.4; $c_{Cl} = 0.1$ mM). To fix the mass concentration of PEG, we used $c_{PEG} = 1$ mM and 2.83 mM for $\theta^*_{Cl} = 0.2$ and 0.4, respectively. The surface concentration at saturation was adjusted correspondingly, i.e. $\Gamma_{PEG}(\theta^*_{Cl} = 0.4) = 2\Gamma_{PEG}(\theta^*_{Cl} = 0.2)$.

A recent in situ STM study[33] showed that the adsorbed PEG has a linear winding shape. Also for this conformation, a smaller value of the threshold θ^*_{Cl} corresponds to a higher value of the PEG molecular weight. Only the value of θ^*_{Cl} is now proportional to M^{-1}_{PEG} instead of $M^{-2/3}_{PEG}$.

Hysteresis mechanism.—The complex hysteresis behavior of our simulated CVs is closely related to the adsorption-desorption kinetics of PEG and chloride and the suppression effect of PEG-Cl complex. In our model, the relationship between the deposition current and the surface coverages of both additives is crucially controlled by the current suppression function $\epsilon(\theta_{PEG})$ in Eq. 7 and the coverage-capacity function $\theta^{max}_{PEG}(\theta_{Cl})$ in Eq. 1. In the following, we study the effect of these functions on the CVs in more detail.

In Fig. 7, the deposition current is presented as a function of the overpotential together with the corresponding variation of the surface coverages θ_{Cl} and θ_{PEG}. During the forward scan (cathodic direction), the surface coverage θ_{PEG} starts to deviate from 1.0 as θ_{Cl} decreases below the threshold value $\theta^*_{Cl} = 0.2$ (cf. the coverage-capacity function $\theta^{max}_{PEG}(\theta_{Cl})$ in Fig. 1a). The jump-like increase of the current i_{Cu} is triggered much later at a critical potential when θ_{PEG} crosses the threshold value $\theta^*_{PEG} = 0.4$. This sudden current change is clearly caused by the cusp in the current suppression function

Downloaded on 2017-06-29 to IP 141.30.233.235 address. Redistribution subject to ECS terms of use (see ecsdl.org/site/terms_use) unless CC License in place (see abstract).

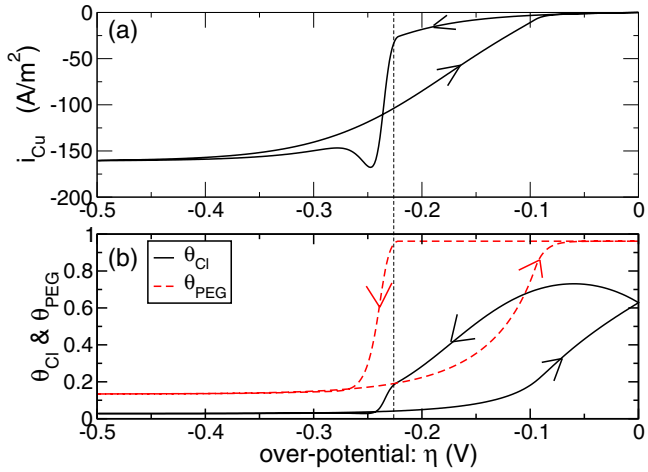

Figure 8. Simulation analogous to Fig. 7, but with $\theta^*_{Cl} = 0.2$ and $\theta^*_{PEG} = 1.0$. In difference to the case in Fig. 7, the steep change in the current density i_{Cu} starts when the surface coverage of chloride θ_{Cl} crosses the value $\theta^*_{Cl} = 0.2$.

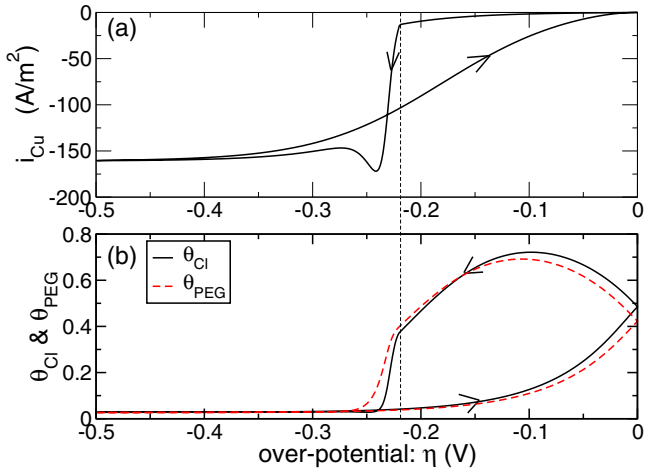

Figure 9. Simulation analogous to Fig. 7, but with $\theta^*_{Cl} = 1.0$ and $\theta^*_{PEG} = 0.4$. The steep change in the current density i_{Cu} starts when the surface coverage of PEG θ_{PEG} crosses the value $\theta^*_{PEG} = 0.4$.

$\epsilon(\theta_{PEG})$ (cf. Fig. 1b). Moreover, a positive feedback between the current increase and the corresponding increased chloride desorption, followed by an increased PEG desorption for $\theta_{PEG} < \theta^*_{PEG}$, results in the observed strong current increase.

During the backward scan, the current changes gradually when crossing the critical potential since at that moment the surface coverage θ_{PEG} is far below the threshold value $\theta^*_{PEG} = 0.4$. Finally, a small kink appears in the current curve when θ_{PEG} crosses again the threshold value 0.4. Note that the overshooting of the current in the forward scan is also observed in experiments.[9] The reason for this phenomenon is the fast decrease of the PEG surface coverage, whereas the concentration of copper ions in the electrolyte near the cathode surface is still high. Afterwards, the copper concentration relaxes to a diffusion-limited value which controls then the deposition current. The amplitude of the overshooting diminishes if a smaller sweeping rate is used, which is related to a stronger depletion of the copper concentration. The surprising non-monotonic variation of θ_{Cl} during the forward scan is related to the finite sweep rate. Obviously, chloride adsorption prevails desorption in the early stage of the forward scan.

The simulation of the CV in Fig. 8 was performed for a value $\theta^*_{PEG} = 1.0$ (fixed $\theta^*_{Cl} = 0.2$). Such a special case, with the suppression function in Eq. 7 becoming linear, resembles the model proposed in Ref. 14. In this case, the jump-like increase of the current during the forward scan occurs when θ_{Cl} crosses the value θ^*_{Cl} and θ_{PEG} starts to deviate from 1.0. Furthermore, Fig. 9 presents the result of a simulation with $\theta^*_{Cl} = 1.0$ and $\theta^*_{PEG} = 0.4$. Here, the transition in the current occurs when θ_{PEG} crosses the value θ^*_{PEG}. By setting both threshold values θ^*_{Cl} and θ^*_{PEG} equal to 1.0, i.e. rendering the functions $\theta^{max}_{PEG}(\theta_{Cl})$ and $\epsilon(\theta_{PEG})$ to be linear, the hysteresis behavior will disappear completely as discussed in Ref. 21. In summary, the simulations in Figs. 7 to 9 indicate that the hysteresis behavior with a jump-like current transition can be generated by each of the two mechanisms alone: either the nonlinearity of the current suppression function $\epsilon(\theta_{PEG})$ in Eq. 7, or the nonlinearity of the coverage-capacity function $\theta^{max}_{PEG}(\theta_{Cl})$ in Eq. 1. Their combination in our model makes it more flexible to produce the hysteresis and enables its wide application to different experimental situations.

A further analysis of our proposed model concerned the impact of the kinetic parameters on the hysteresis behavior of CVs. As shown in Fig. 10, the appearance of hysteresis is generic for a wide range of parameter values. The change in the shape of the CVs with varying parameters reflects the sensitivity of the hysteresis behavior with respect to those parameters. Interestingly, variation of parameter k^{Cl}_d does not noticeably influence the CV for the used parameter set. It indicates possibly a negligible contribution of the normal thermally activated Cl^- desorption compared to the deposition-activated desorption.

In our preceding simulations, we have always used a cusp-like form of the capacity and suppressor functions as shown in Fig. 1. Such a form appears somewhat artificial. It is therefore interesting to study the effect of a smooth curve progression of these functions on the hysteresis behavior. Examples of such smooth functions are also shown in Fig. 1 ($\theta^{max}_{PEG}(\theta_{Cl}) = 1 - \exp(-5\theta_{Cl})$ and $\epsilon(\theta_{PEG}) = \exp(-5\theta_{PEG})$). In Fig. 11, simulated CVs for the two cases with piecewise-linear and smooth functions are compared. As expected, the sudden increase of the current during the forward scan occurs more gradually for the smooth functions, but it is still rather steep. The smoother curve progression of the CV resembles more experimental CV measurements.[9,14] This comparison indicates that the nonlinearity of the coverage-capacity and suppression functions is the fundamental origin of the hysteresis behavior, not the cusp-like form.

Comparison with previous models.—The model proposed here is closely related to modeling approaches in Refs. 14, 26. Considering the very large molecular size of PEG compared to chloride, Hebert argued that a fractional Cl^- coverage is already sufficient to reach complete coverage of copper by PEG.[26] Within our model, this corresponds to the introduction of the coverage-capacity function $\theta^{max}_{PEG}(\theta_{Cl})$, in Eq. 1 (cf. Fig. 1a). The modeling in Ref. 26 was able to reproduce the hysteresis in CVs by assuming additive incorporation in the deposit. To our knowledge, the first model, which predicts hysteresis without including additive consumption, was proposed by Yang et al.[14] In their stochastic modeling approach, they also assumed the existence of a fractional Cl^- coverage for complete PEG coverage. Adsorption and desorption of PEG was assumed to proceed in multiple steps and master equations were used to describe the probabilistic transition between different adsorption states.

Another crucial ingredient in our model is the current suppression function $\epsilon(\theta_{PEG})$ in Eq. 7. Introduction of this function was motivated by PEG desorption experiments by Willey and West,[31] which revealed a two-stage desorption behavior of PEG (cf. also Appendix). This characteristic behavior was not taken into account in the modeling approaches by Hebert[26] and by Yang et al.[14] In this respect, their model assumptions correspond to the special case $\theta^*_{PEG} = 1.0$ in our model. The simulated CVs in Figs. 8 and 9 demonstrate that the strongly nonlinear coverage-capacity function as well as the suppression function alone are able to reproduce the hysteresis of CVs under certain conditions. It is expected that the combined incorpo-

Downloaded on 2017-06-29 to IP 141.30.233.235 address. Redistribution subject to ECS terms of use (see ecsdl.org/site/terms_use) unless CC License in place (see abstract).

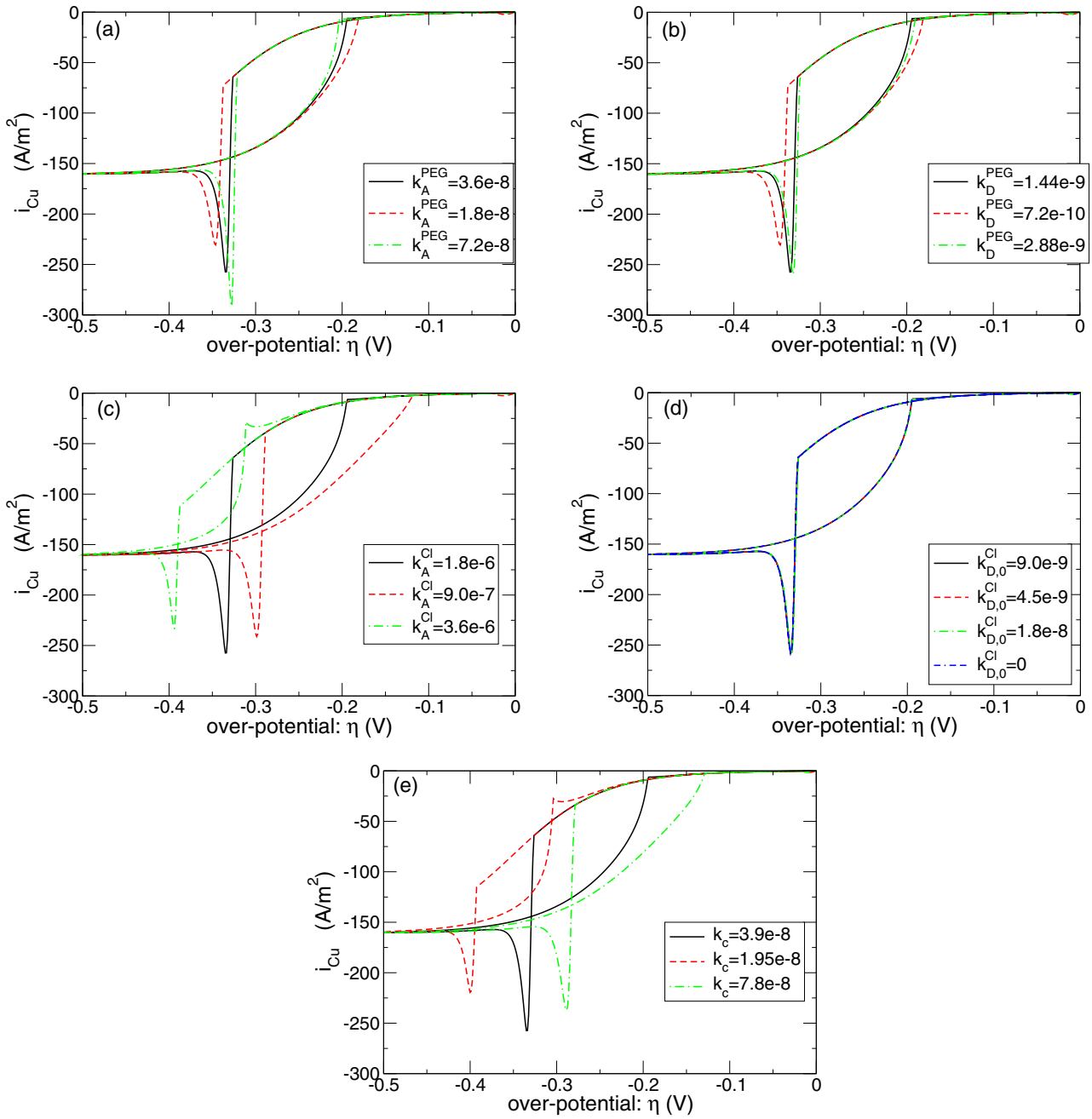

Figure 10. Overview of the impact of kinetic model parameters on CVs: adsorption (a) and desorption (b) rate constant of PEG, adsorption (c) and desorption (d) rate constant of chloride, and coefficient of the deposition-activated desorption of chloride k_c (e), see Eq. 4. Diagram (d) reveals that the desorption rate constant of chloride has very little effect on the CV ($c_{Cl} = 0.1$ mM, $c_{PEG} = 1$ mM, for other parameters see Table I).

ration of these tow factors in our model would widen its scope of application.

Conclusions

We proposed a new model for the electrochemical deposition of copper in the presence of PEG and chloride in the electrolyte. Two characteristic functions were surmised to describe the coadsorption of PEG and chloride and the current-suppression effect of the formed additive complexes. In view of the large size of PEG molecules compared to chloride, a critical fraction of the chloride coverage is assumed to be sufficient for the complete coverage of the copper surface by PEG. The suppression effect of PEG is captured by a more realistic nonlinear function inferred from PEG desorption experiments, in contrast to the commonly used linear relation between deposition current and PEG coverage. Instead of assuming the consumption of additives due to degradation or incorporation in deposits, we supposed an additional activation of additive desorption caused by the copper deposition, as originally proposed in Ref. 14. Based on these suppositions, our model is able to reproduce a series of specific features of CVs and adsorption-desorption measurements reported in the literature. Especially, without invoking the consumption of additives, our simple model reproduces the observed hysteresis in CVs and the accompanying sharp transition in the current suppression. We think that the newly incorporated nonlinear current suppression effect of additive complexes, the mathematical simplicity of our model and its robustness with respect to parameter changes make it suited for a wide application in future studies.

Downloaded on 2017-06-29 to IP 141.30.233.235 address. Redistribution subject to ECS terms of use (see ecsdl.org/site/terms_use) unless CC License in place (see abstract).

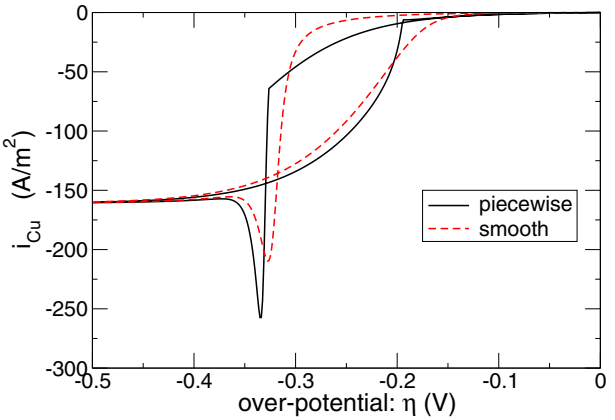

Figure 11. Comparison of simulations of CVs using piecewise-linear and smooth functions $\theta_{PEG}^{max}(\theta_{Cl})$ and $\epsilon(\theta_{PEG})$ (see Fig. 1 and Eqs. 1 and 7, $c_{Cl} = 0.1$ mM, $c_{PEG} = 1$ mM). By using smooth functions, the transition in the current density becomes rounded, similar to experimental results in Refs. 10, 14, 26.

Acknowledgments

This work was funded by the EFRE fund of the European Community and by funding of the State of Saxony of the Federal Republic of Germany, project EVOLVE (project number 100218333), and is supported by the Dresden Center for Computational Materials Science (DCCMS). We also acknowledge the support by the German Research Foundation (DFG) within the Cluster of Excellence "Center for Advancing Electronics Dresden" (cfAED). We acknowledge the Center for Information Services and High Performance Computing (ZIH) at TU Dresden for computational resources. The authors thank Axel Preusse, Romy Liske, Robert Krause and other partners of the project EVOLVE for helpful discussions.

Appendix: Current Suppression Function

Willey and West[31] observed that the desorption of PEG proceeds in two stages: in the first stage the deposition current shows a slow linear increase, followed by an exponential increase in the second stage (cf. Fig. 2, black curve). In the following, we argue how the current suppression function established in Eq. 7 can be inferred from the time dependence of the measured deposition current. In general, the change of the exchange current can be expressed as

$$i_0^{PEG}(t) = \epsilon(t) i_0^{free}. \qquad [A1]$$

similarly to Ref. 21, but with a time-dependent current reduction ratio $\epsilon(t)$. According to Eq. A1, the slow initial current change can be described by a linear variation of $\epsilon(t)$

$$\epsilon(t) = \epsilon_0 - (\epsilon_0 - \epsilon_1)\frac{t}{t^*}, \qquad [A2]$$

where ϵ_0 is the current reduction ratio at the PEG surface coverage $\theta_{PEG} = 1$ (at $t = 0$), and ϵ_1 the ratio at $\theta_{PEG} = \theta_{PEG}^*$, i.e. at the transition point to the second stage $t = t^*$. According to Ref. 31, the linear increase of the deposition current in the first desorption stage could be caused by a decrease of the adsorption layer thickness of PEG. Assuming a linear decrease of the PEG coverage, this leads to

$$\theta_{PEG}(t) = 1 - (1 - \theta_{PEG}^*)\frac{t}{t^*}. \qquad [A3]$$

Elimination of t/t^* from Eqs. A2 and A3 yields

$$\epsilon = \epsilon_0 - (\epsilon_0 - \epsilon_1)\frac{1 - \theta_{PEG}}{1 - \theta_{PEG}^*}. \qquad [A4]$$

In the second desorption stage, the adsorption layer becomes more and more patchy with time. Since the electrolyte is kept free of additives via a specially designed microfluidic device, back-adsorption of desorbed PEG molecules is negligible. PEG desorption is then simply described by

$$\frac{d\theta_{PEG}}{dt} = -k\theta_{PEG} \qquad [A5]$$

with k as desorption rate constant. This leads to an exponential decrease of the surface coverage with time

$$\theta_{PEG}(t) = \theta_{PEG}^* e^{-k(t-t^*)}. \qquad [A6]$$

Correspondingly, the exponential increase of the exchange current density (observed in Ref. 31) can be described by

$$i_0^{PEG}(t) = \left\{1 - (1 - \epsilon_1)e^{-k(t-t^*)}\right\} i_0^{free}. \qquad [A7]$$

Elimination of the exponential term from Eqs. A6 and A7 yields

$$\frac{i_0^{PEG}}{i_0^{free}} = 1 - (1 - \epsilon_1)\frac{\theta_{PEG}}{\theta_{PEG}^*}. \qquad [A8]$$

By combining Eqs. A1, A4, and A8, one finally finds the current suppression function Eq. 7.

References

1. P. C. Andricacos, C. Uzoh, J. Dukovic, J. Horkanes, and H. Deligianni, *IBM J. Res. Dev.*, **42**, 567 (1998).
2. K. Kondo, R. N. Akolkar, D. P. Barkey, and M. Yokoi, Editors, *Copper Electrodeposition for Nanofabrication of Electronics Devices*, Springer, 2014.
3. Z. Nagy, J. P. Blaudeau, N. C. Hung, L. A. Curtiss, and D. J. Zurawski, *J. Electrochem. Soc.*, **142**, L87 (1995).
4. J. J. Kelly and A. C. West, *J. Electrochem. Soc.*, **145**, 3477 (1998).
5. M. L. Walker, L. J. Richter, and T. P. Moffat, *J. Electrochem. Soc.*, **152**, C403 (2005).
6. W.-P. Dow and H.-S. Huang, *J. Electrochem. Soc.*, **152**, C67 (2005).
7. Z. V. Feng, X. Li, and A. A. Gewirth, *J. Phys. Chem. B*, **107**, 9415 (2003).
8. K. Doblhofer, S. Wasle, M. Soares, K. G. Weil, and G. Ertl, *J. Electrochem. Soc.*, **150**, C657 (2003).
9. V. D. Jović and B. M. Jović, *J. Serb. Chem. Soc.*, **66**, 935 (2001).
10. B.-H. Wu, C.-C. Wan, and Y.-Y. Wang, *J. Appl. Electrochem.*, **33**, 823 (2003).
11. M. E. Huerta Garrido and M. D. Pritzker, *J. Electrochem. Soc.*, **155**, D332 (2008).
12. M. E. Huerta Garrido and M. D. Pritzker, *J. Electrochem. Soc.*, **156**, D36 (2009); **156**, D175 (2009).
13. L. Yang, A. Radisic, J. Deconinck, and P. M. Vereecken, *J. Electrochem. Soc.*, **160**, D3051 (2013).
14. L. Yang, A. Radisic, J. Deconinck, and P. M. Vereecken, *J. Electrochem. Soc.*, **161**, D269 (2014).
15. T. P. Moffat and D. Josell, *J. Electrochem. Soc.*, **159**, D208 (2012).
16. S.-K. Kim, D. Josell, and T. P. Moffat, *J. Electrochem. Soc.*, **153**, C616 (2006).
17. S.-K. Kim, D. Josell, and T. P. Moffat, *J. Electrochem. Soc.*, **153**, C826 (2006).
18. D. Josell, D. Wheeler, and T. P. Moffat, *J. Electrochem. Soc.*, **159**, D570 (2012).
19. D. Wheeler, T. P. Moffat, and D. Josell, *J. Electrochem. Soc.*, **160**, D3260 (2013).
20. D. Josell and T. P. Moffat, *J. Electrochem. Soc.*, **163**, D322 (2016).
21. D. Roha and U. Landau, *J. Electrochem. Soc.*, **137**, 824 (1990).
22. R. Akolkar and U. Landau, *J. Electrochem. Soc.*, **151**, C702 (2004).
23. R. Akolkar and U. Landau, *J. Electrochem. Soc.*, **156**, D351 (2009).
24. E. Rusli, F. Xue, T. O. Drews, P. Vereecken, P. Andracacos, H. Deligianni, R. D. Braatz, and R. C. Alkire, *J. Electrochem. Soc.*, **154**, D584 (2007).
25. K. R. Hebert, *J. Electrochem. Soc.*, **148**, C726 (2001).
26. K. R. Hebert, *J. Electrochem. Soc.*, **152**, C283 (2005).
27. R. Liske, Ph.D. Thesis, TU Dresden, (2009).
28. R. Liske, R. Krause, B. Uhlig, L. Gerlich, S. Bott, M. Wislicenus, and A. Preusse, *J. Electrochem. Soc.*, **163**, D213 (2016).
29. M. Kang and A. A. Gewirth, *J. Electrochem. Soc.*, **150**, C426 (2003).
30. M. Hayase, M. Taketani, K. Aizawa, T. Hatsuzawa, and K. Hayabusa, *Electrochem. Solid-State Lett.*, **5**, C98 (2002).
31. M. J. Willey and A. C. West, *J. Electrochem. Soc.*, **153**, C728 (2006).
32. V. G. Levich, *Physicochemical Hydrodynamics*. Englewood Cliffs, NJ (1962).
33. L.-H. Li, S. Yau, and W.-P. Dow, *Electrochem. Commun.*, **70**, 1 (2016).

Downloaded on 2017-06-29 to IP 141.30.233.235 address. Redistribution subject to ECS terms of use (see ecsdl.org/site/terms_use) unless CC License in place (see abstract).